

# Elements Selection for Auxiliary Array in the Adaptive Sidelobe Canceller Radar System

Jafar Ramadhan Mohammed<sup>1\*</sup>

<sup>1</sup> Department of Communication Engineering, College of Electronics Engineering, Ninevah University, Al-Jawsaq, Right Coast, 41002 Mosul, Iraq

\* Corresponding author, e-mail: [jafar.mohammed@uoninevah.edu.iq](mailto:jafar.mohammed@uoninevah.edu.iq)

Received: 13 May 2022, Accepted: 20 September 2022, Published online: 05 October 2022

## Abstract

In a recent paper, the conventional sidelobe canceller radar system was developed by replacing the separate auxiliary antennas by few elements at the center of the main antenna array. The modified system with reused elements was associated with some attenuation in the desired signal due to the emerging correlation between the signals that exists in the main and the reused array elements. This problem was solved by imposing some constraints on the array pattern of the reused elements. In this paper, few of the side elements of the main array are employed as the auxiliary antennas. This new proposed configuration is called sided-elements. Unlike the previous centered-elements configuration, the proposed sided-elements configuration offers more desired features since the pattern of the side elements has sidelobes of similar widths of those of the main array. Moreover, a better diversity is obtained due to the wider separation between the two groups of elements at both sides of the main array. Simulation results fully confirm the effectiveness of the new proposed sided-elements configuration for suppressing the undesired interfering signals and retaining the desired signal undistorted.

## Keywords

radar system, adaptive arrays, sidelobe canceller, auxiliary antennas, reused elements, interference suppression

## 1 Introduction

In the conventional adaptive sidelobe canceller system, the interfering signal incident on the sidelobes of the main antenna is cancelled by generating a signal of equal magnitude and antiphase using a separate auxiliary antenna configuration [1]. The separate auxiliary array configuration has many disadvantages such as high complicated system, needs more RF components, and costly. Other inherent disadvantage is the cancellation of the desired signal which usually occurs when the desired signal present in the main array and leaks into the auxiliary antennas during the normal operation of the radar system [1–4]. The adaptation process determines the weights of the auxiliary antenna elements by minimizing the total output power. Thus, the cancellation percentage increases with stronger desired signal that contributes in a higher percentage in the total output power. This problem may be solved by applying some linear constraints to the weight vector of the auxiliary antenna as in the well-known minimum variance distortionless response (MVDR) beamformer [5, 6]. However, the standard MVDR beamformer

is only active under perfect steering vector and without any implementation errors [7, 8] which is impractical.

Recently, several efficient null steering methods have been proposed based on either modifying the amplitude and the phase excitations of few selected elements [9–12] or controlling their positions [13] or even controlling the weight perturbation of the array elements [14].

In this paper, various auxiliary configurations are investigated to determine how the reutilized array elements should be selected to provide good cancellation of interfering signals while retaining low sidelobe levels in the main array pattern. The proposed configuration involves the reuse of few elements at both sides of the original array, to form as the auxiliary antenna that is used to produce the required cancellation pattern. This approach offers a lower cost since no separate auxiliary antennas is needed. The amplitude and phase excitations of the reused auxiliary elements are adaptively adjusted such that they produce a pattern that coincides in antiphase with one or more sidelobe of the original array pattern. A deep null or nulls

toward the interfering signals can thus be generated in the resulting pattern. For a good performance, the cancellation pattern should have minimal level along the direction of desired signal to keep the level of the desired signal unchanged. In the proposed sided-elements configuration, the correlation between signals in the main and auxiliaries is relatively small since only few side elements which are a small fraction of the total array elements are reused for the auxiliaries. Moreover, the side elements which are located at the ends of the array have usually small weights in the array amplitude taper.

This paper is organized as follows. Section 2 briefly describes the system model of the conventional adaptive sidelobe canceller, while Section 3 presents the proposed strategy that can be used to find how the reused elements should be chosen for the auxiliary array in the modified sidelobe canceller system while attaining best performance. In Section 4, the obtained results of the simulations are provided to demonstrate the performance of the proposed technique and concluding remarks are given in Section 5.

## 2 Conventional adaptive sidelobe canceller

Fig. 1 shows the conventional adaptive SLC system consisting of a main array with  $N$  elements,  $M$  separate auxiliary elements, and the adaptive control. Usually,  $N$  is much higher than  $M$ , thus the gain of the main array is much higher than that of the auxiliary array. Assume a desired source with waveform denoted by  $d(k)$  is incident from direction  $\theta_d$  and a number of interfering signals,  $P$ , with waveforms denoted by  $i_1, i_2, \dots, i_p$  are incident from

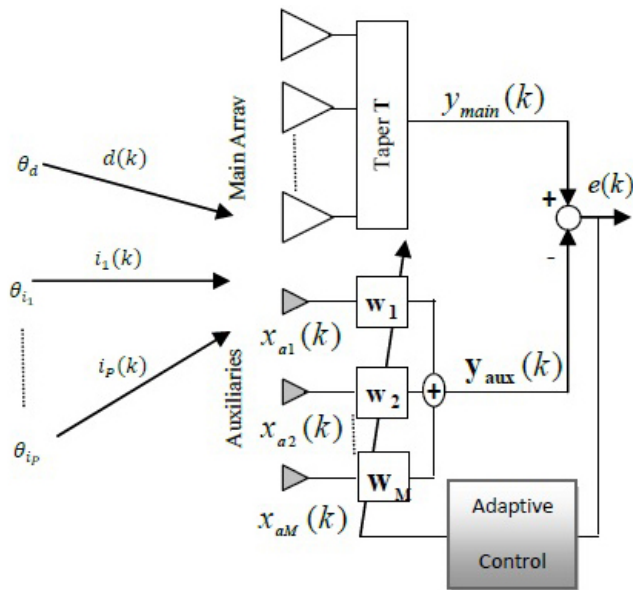


Fig. 1 Conventional SLC with separate auxiliaries

angles  $\theta_{i_1}, \theta_{i_2}, \dots, \theta_{i_p}$ . The total received signal on any array elements, say element  $n$ , can be given by

$$y_n(k) = d_n(k) + \sum_{p=1}^P i_n^p + g_n(k), \quad (1)$$

where  $g_n(k)$  is the zero mean Gaussian noise for each element.

The highly directional beam of the main array is pointed towards the desired signal source, while the interfering signals are usually incident through the sidelobes of the main array pattern, and at the same time they incident on the auxiliaries. The amplitude taper,  $T$ , of the main array can be chosen such that the main array pattern has maximum gain at desired direction  $\theta_d$  and low sidelobes at other undesired directions. In this paper, we use both uniform and nonuniform such as Dolph tapers. The output of the main channel after tapering is

$$y_{\text{main}}(k) = \sum_{n=1}^N T_n e^{-j \frac{2\pi}{\lambda} d(n-1) \sin(\theta_d)}, \quad (2)$$

where the phase factor in Eq. (2) steers the main beam toward desired angle  $\theta_d$  and the weights  $T_n$  provide the required amplitude taper across the main array elements. Whereas the output of the auxiliary channel is

$$y_{\text{aux}}(k) = W_a^H(k) x_a(k), \quad (3)$$

where  $W_a = [w_1, w_2, \dots, w_M]^T$  are the adaptive weights of the auxiliary elements and  $x_a$  are their input signals. In order to place the desired nulls toward the interfering signals at the sidelobe regions of the main array pattern, the auxiliary weights need to be properly determined. This requires that the sidelobe pattern of the main array in the directions of the interfering signals and that of the auxiliary array are kept in same level and in antiphase resulting in an overall system response of zero at the direction of interference signal. In this paper, the least mean squares (LMS) algorithm [15, 16] is used to adaptively update the weights of the auxiliaries according to the following error function:

$$e(k) = y_{\text{main}}(k) - y_{\text{aux}}(k). \quad (4)$$

Then, the LMS solution is

$$W_a(k+1) = W_a(k) + \mu e^*(k) x_a(k), \quad (5)$$

where  $\mu$  is the step-size parameter that controls the convergence speed of the LMS algorithm. There are some inherent disadvantages with this configuration as shown below, when signal to interference-plus-noise ratio (SINR) gets stronger more signal leaks through the auxiliaries. As a

result, the output signal of the auxiliaries will contain a significant amount of desired signal as well as the interfering signals. Choosing proper weight values,  $W_a$ , to minimize the output power may lead to cancellation of the desired signal beside the interfering signals. Therefore, cancellation of the desired signal in this configuration is inevitable. Thus, a need for a separate auxiliary array becomes unnecessary and impractical. Replacing them with some existing elements in the main array may offer a simpler and less expensive configuration as can be seen in Section 3.

### 3 The modified sidelobe canceller

The structure of the reused central-elements configuration was investigated in [17]. However, the selection of the central elements as the auxiliaries does not provide best performance. A new configuration of the SLC system with the side-elements as the auxiliaries is suggested in this paper. Its configuration is shown in Fig. 2 where instead of using few elements at the center of the main array for the auxiliary array function, the auxiliary array here is formed by few elements symmetrically located at both sides of the main array. The first step in the proposed technique is to generate a cancellation pattern from the chosen elements. The second step is to place a null in the resulting array pattern by subtracting the cancelation pattern from the main array pattern. More than one null can be placed in the resulting pattern by properly weighting the amplitude and the phase excitations of the side elements. The optimal weights of the reused side elements are obtained by using the LMS that was presented by Eq. (5). The details of each step are shown in Sections 3.1–3.3.

### 3.1 The main array pattern

The elements of the main array are assumed as scalar isotropic receivers for a simpler description of the idea, while in the practical design, the element pattern and polarization can then be accounted for. For an  $N$ -element array of fixed inter-element spacing  $d$ , the far field pattern is given by

$$AF_{Main}(\theta) = \sum_{n=1}^N T_n e^{j\left[\frac{2\pi}{\lambda}d(n-1)\sin(\theta)+\beta\right]}, \quad (6)$$

where  $\theta$  is the angular position of the field point which measured from broadside to the array axis, and  $\beta$  is the progressive phase difference between adjacent elements that is necessary to direct the main beam to an angle  $\theta_d$ .

### 3.2 The auxiliary array pattern

Let the auxiliary array under investigation is composed of  $M$  elements of the main array that are symmetrically located at both sides of the  $N$ -element main array as shown in Fig. 2. The radiated field by the auxiliary array can be considered as the summation of pairs of elements that are separated by distances of  $(N - 1)d$ ,  $(N - 3)d$ ,  $(N - 5)d$ , ..., and so on. Starting from the pair having the 1<sup>st</sup> and  $N^{\text{th}}$  elements which are placed at the extreme ends of the array. Let the complex weights of the excitations of the  $M$  auxiliary elements be  $W_a$ , and thus it can be written as

$$W_a = [w_1, w_2, \dots, w_{M/2}], \quad (7)$$

where  $w_m = b_m e^{j\alpha_m}$  is the magnitude,  $b_m$ , and phase,  $\alpha_m$ , excitations of the  $m^{\text{th}}$  pair of elements. Then, the auxiliary array pattern is given by

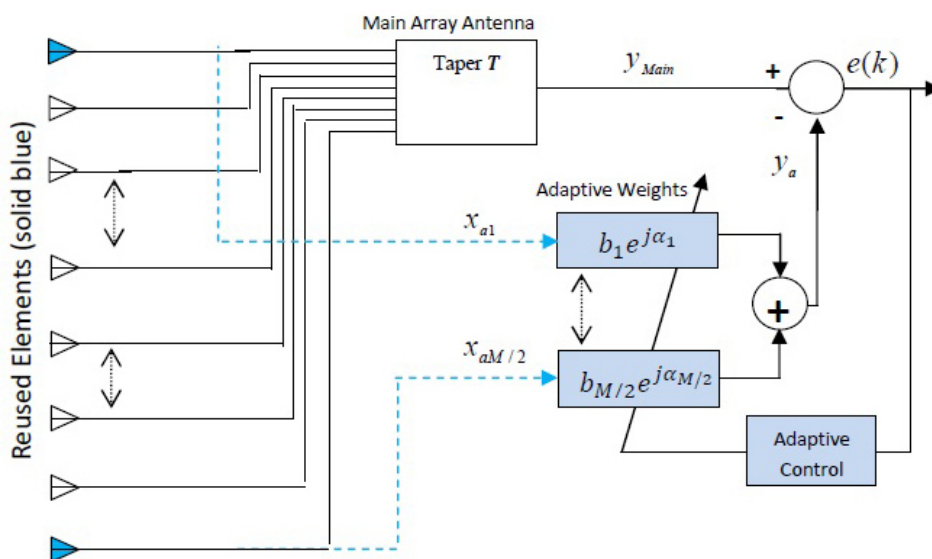


Fig. 2 Proposed SLC system with side-elements configuration

$$AF_{\text{Auxiliary}}(\theta) = \sum_{m=1}^{M/2} 2b_m \times \cos\left[\left(N - (2m-1)\right)\pi d/\lambda \sin(\theta) + \alpha_m\right] \quad (8)$$

This pattern is a summation of cosine patterns where each pattern is in the form of sidelobes having a constant level  $2b_m$ . This feature will be utilized to place the required nulls in the pattern of the main array.

The total far field pattern due to the sum of the main and the auxiliary array patterns is

$$AF_{\text{Adapted}}(\theta) = AF_{\text{Main}}(\theta) + AF_{\text{Auxiliary}}(\theta) \quad (9)$$

$$AF_{\text{Adapted}}(\theta) = \sum_{n=1}^N T_n e^{j\left[\frac{2\pi}{\lambda} d(n-1)\sin(\theta) + \beta\right]} + \sum_{m=1}^{M/2} 2w_m \cos\left[\left(N - \left(\frac{2m-1}{2}\right)\right)\frac{2\pi}{\lambda} d \sin(\theta)\right] \quad (10)$$

The goal is to choose the complex weights  $w_m$  of the reused auxiliary sided-elements in order to place  $P$  adaptive nulls in the directions of interfering signals,  $\theta_{i_p}$ , which is expressed as

$$AF_{\text{Adapted}}(\theta)\Big|_{\theta=\theta_{i_p}} = 0 \quad (11)$$

This requires that the magnitudes of the cancellation pattern (2<sup>nd</sup> term of Eq. (10)) and the main array pattern (1<sup>st</sup> term of Eq. (10)) to be equal in magnitude and in antiphase at the location of each of the nulls. This condition is necessary to force the total field in the far field zone to be zero or minimal at the direction of the interference signal. This can be achieved by proper determination of the parameters ( $b_m$  and  $\alpha_m$ ) for the given values of  $N$ ,  $M$ , and  $\theta_{i_p}$  ( $p = 1, 2, \dots, P$ ).

### 3.3 The performance measures

The first performance measure of the overall modified SLC system is the peak main beam reduction which can be computed from Eq. (10) after substituting the desired signal direction  $\theta_d$ . Assuming the main beam peak is in the broadside direction  $\theta = \theta_d = 0^\circ$ , then the peak main beam reduction in the broadside direction is

$$\text{Main beam reduction} = AF_{\text{Adapted}}(0) = \sum_{n=1}^N T_n - \sum_{m=1}^{M/2} 2w_m \quad (12)$$

For uniformly excited arrays, the first term in Eq. (12) becomes  $N$ . The second term in Eq. (12) represents the reduction in the level of the main beam from its original value before the adaptation process is called as the reduction factor. Note that the reduction factor is directly proportional to the number of the reused auxiliary elements.

Thus, a relatively higher main beam reduction has to be tolerated when it is required to generate more nulls.

The second performance measure is the average sidelobe level (ASL) of an array pattern where it is defined as the integral of the array radiation pattern over the sidelobe region. The ASL of the resultant pattern that given in Eq. (10) can be determined as

$$ASL_{\text{Adapted}} = \int_{\theta_{sl}} |AF_{\text{Adapted}}(\theta)|^2 \sin(\theta) d\theta \quad (13)$$

where  $\theta_{sl}$  denotes the sidelobe region. For comparison, the ASL of the main array pattern can be also computed by the same manner. Then the difference between  $ASL_{\text{Adapted}} - ASL_{\text{main}}$  represents an increase in the ASL.

The other performance measure is the directivity which is computed by [18]:

$$\text{Directivity}_{dB} = 10 \text{Log}_{10} \left( \frac{4\pi U_{\text{Adapted}}(\theta)}{P_{\text{rad}}} \right) \quad (14)$$

where  $U_{\text{Adapted}}(\theta) = [AF_{\text{Adapted}}(\theta)]^2$  is the radiation intensity of the resultant array with adapted side-elements and  $P_{\text{rad}}$  is its radiated power.

## 4 Simulation results

In this section, a number of cases are investigated to evaluate the performances of the conventional separate auxiliaries SLC and the two modified SLCs with centered and sided reused-elements configurations. The main array considered is a 20-element with uniform half-wavelength inter-element spacing. The outputs of the main array elements were tapered and summed to form a desired main beam pattern with required low sidelobes. The direction of the desired signal is assumed to arrive at  $0^\circ$  from the broadside direction. Let the desired signal-to-noise ratio per element be  $\text{SNR} = -10$  dB and the interference-to-noise ratio per element be  $\text{INR} = 30$  dB. The  $M$  reused auxiliaries were connected to an adaptive control as shown in Fig. 2 to generate the required cancellation pattern. The weights of the reused auxiliary elements were adaptively adjusted by minimizing the mean square error of the total output power.

In the first example, a single interfering signal that arrives at angle  $\theta_{i_1} = 40^\circ$  and uniform amplitude tapering of the main array are considered. The SNR and the INR values were as mentioned in above. For the sided-element SLC configuration, two elements one at each side of the main array are reused as the auxiliary array. Whereas, for centered-element SLC configuration, the two centered elements of the main array are reused as the auxiliaries.

Fig. 3 (a) shows the patterns of the main array with uniform tapering, cancellation pattern of the auxiliary elements, and the overall adapted pattern of the modified SLC with centered-element configuration for SNR = -10 dB and INR = 30 dB. Whereas Fig. 3 (b) shows the results of the modified SLC with sided-element configuration under the same condition as previous.

From Fig. 3 (a) and (b), it can be seen that the overall adapted patterns of the two modified SLC configurations achieve deep nulls at the interferer direction ( $\theta_i = 40^\circ$ ). More important, the sided-elements configuration provides a pattern with much lower sidelobes with compared to that of the centered-elements configuration. This is mainly because that the pattern of the side elements has sidelobes of similar widths of those of the main array and also because of a better diversity is obtained due to the wider separation between the two groups of elements at both sides of the main array.

The performance measures of these two configurations are listed in Table 1. From Table 1, it can be seen that the performance of the sided-elements configuration

is generally better than that of the centered-elements configuration. Moreover, the mean squared error convergence of these two configurations is illustrated in Fig. 4.

In the second example, non-uniform Dolph-Chebyshev amplitude tapering for the main array is considered. For fair comparison, the number of the auxiliaries and the direction of the interfering signal were same as in the previous example. Fig. 5 and Table 2 show the results of the centered-elements and sided-elements configurations.

From Fig. 5 (b), it can be seen that the cancellation pattern of the auxiliary sided-elements and the original pattern of the main array are completely match in width and levels of the corresponding sidelobes. Thus, the average sidelobe level of the adapted pattern has significantly reduced with compared to that of the original main array. Moreover, the directivity and the peak beam reduction of the modified SLC pattern with sided-elements configuration have been slightly reduced. Furthermore, the taper efficiency of the proposed configuration is acceptable. These results fully confirm the effectiveness of the proposed SLC system with sided-elements configuration.

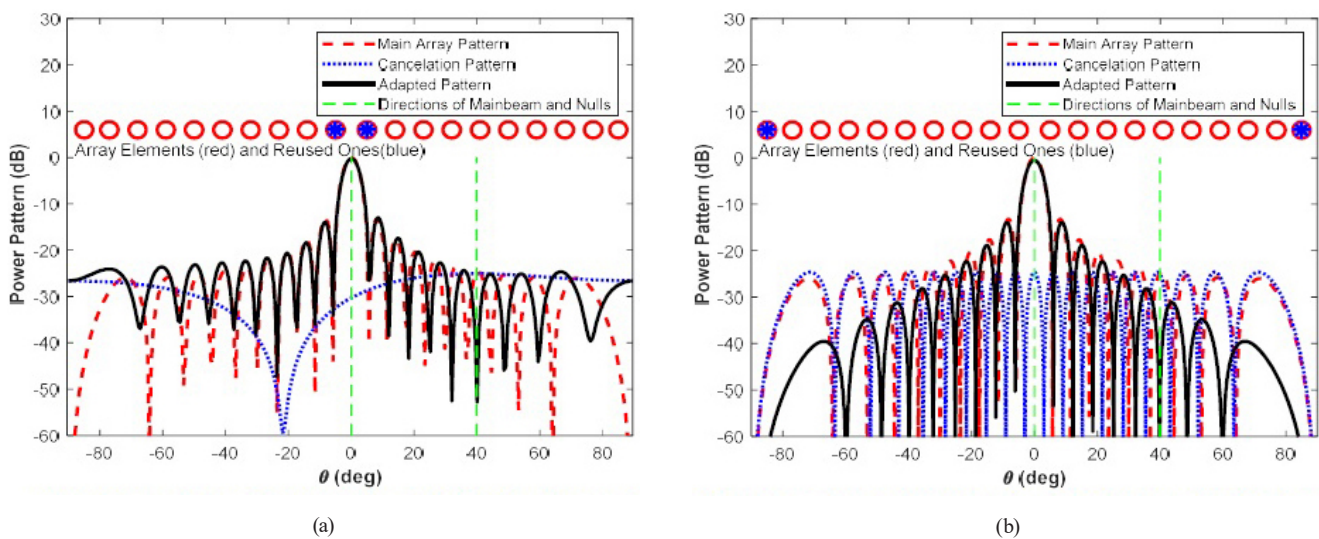


Fig. 3 Power patterns of the main, auxiliary and adapted arrays, for uniform taper,  $N = 20$ ,  $M = 2$ , and a single null, (a) centered-elements configuration, and (b) sided-elements configuration

Table 1 Performance comparison of the tested methods of example 1

Methods	Peak Beam Reduction [dB]	Average-SLL [dB]	Taper Efficiency	Peak SLL [dB]	Directivity [dB]	HPBW [Deg.]	Output SINR [dB]
Main Array with Uniform Taper	0	-21.895	1	-13.2	13.021	5.04	-15.26
Modified SLC with Centered-Elements Configuration	-0.507	-20.905	1.110	-12.9	12.882	4.8	29.967
Modified SLC with Sided-Elements Configuration	-0.140	-23.288	1.111	-14.0	12.861	4.9	45.175



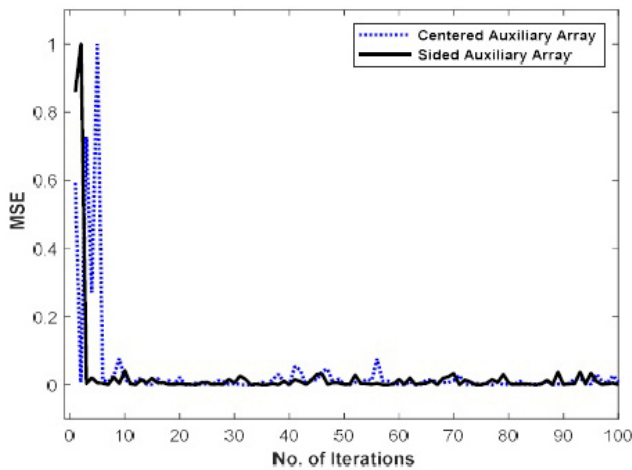
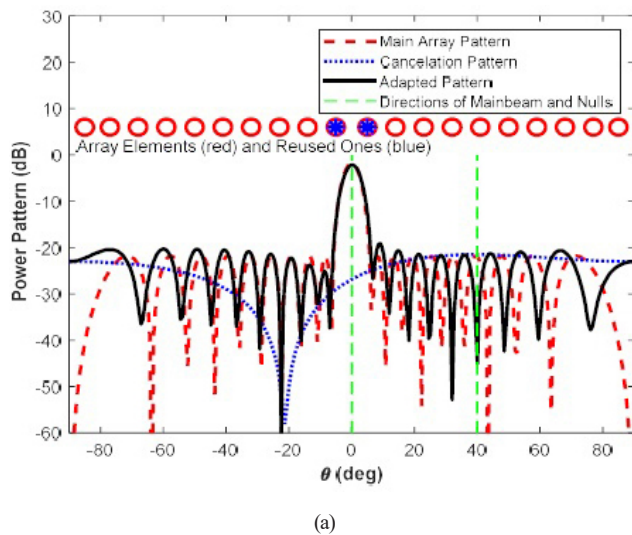


Fig. 4 Mean Squared Errors (MSE) versus iteration number for  $N = 20$ ,  $M = 2$ , and a single null

In the third example, the performances in terms of main beam reduction, average sidelobe level, directivity



and the output SINR of the two considered configurations under various interferer power values are investigated. Fig. 6 (a)–(d) shows the results. In this case, the Dolph taper with  $SLL = -20$  dB, single null at  $40^\circ$ , two auxiliary elements, and  $SNR = -10$  dB were considered. Generally, it is observed that the performance measures are greatly relying on the auxiliary elements location where the average SLL is most distorted when the auxiliary elements are at the center of the main array and least distorted when they are at the sides.

In the next example, we investigate how the main beam reduction and the directivity of the two configurations change with the number of reused auxiliaries under fixed value of the interferer power  $INR = 30$  dB and  $SNR = -10$  dB. Other parameters were the Dolph taper with  $SLL = -20$  dB and a single null at  $40^\circ$ . Fig. 7 (a) and (b) shows the results.

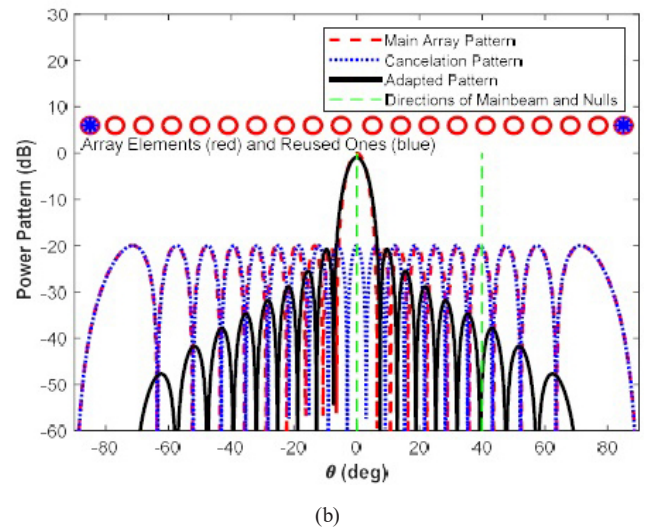


Fig. 5 Power patterns of the main, auxiliary and adapted arrays, for Dolph taper,  $N = 20$ ,  $M = 2$ , and a single null, (a) centered-elements configuration, and (b) sided-elements configuration

Table 2 Performance comparison of the tested methods of example 2

Methods	Peak Beam Reduction [dB]	Average-SLL [dB]	Taper Efficiency	Peak SLL [dB]	Directivity [dB]	HPBW [Deg.]	Output SINR [dB]
Main Array with Dolph Taper and its Weights	0	-20.381	1.522	-20.0	12.797	5.36	-8.385
	$[w_1, \dots, w_{N/2}] = [1.0281, 0.4769, 0.5700, 0.6615, 0.7479, 0.8260, 0.8926, 0.9452, 0.9815, 1.0000]$						
Modified SLC with Centered-Elements Configuration and its Weights	-0.67	-19.061	1.778	-19.0	12.502	5.0	25.449
	$[w_1, \dots, w_{N/2}] = [1.0281, 0.4769, 0.5700, 0.6615, 0.7479, 0.8260, 0.8926, 0.9452, 0.9815, 0.032 - j 0.009]$						
Modified SLC with Sided-Elements Configuration and its Weights	-0.0538	-24.646	1.796	-21.0	12.565	5.1	46.235
	$[w_1, \dots, w_{N/2}] = [0.206 - j 0.0028, 0.4769, 0.5700, 0.6615, 0.7479, 0.8260, 0.8926, 0.9452, 0.9815, 1.0000]$						

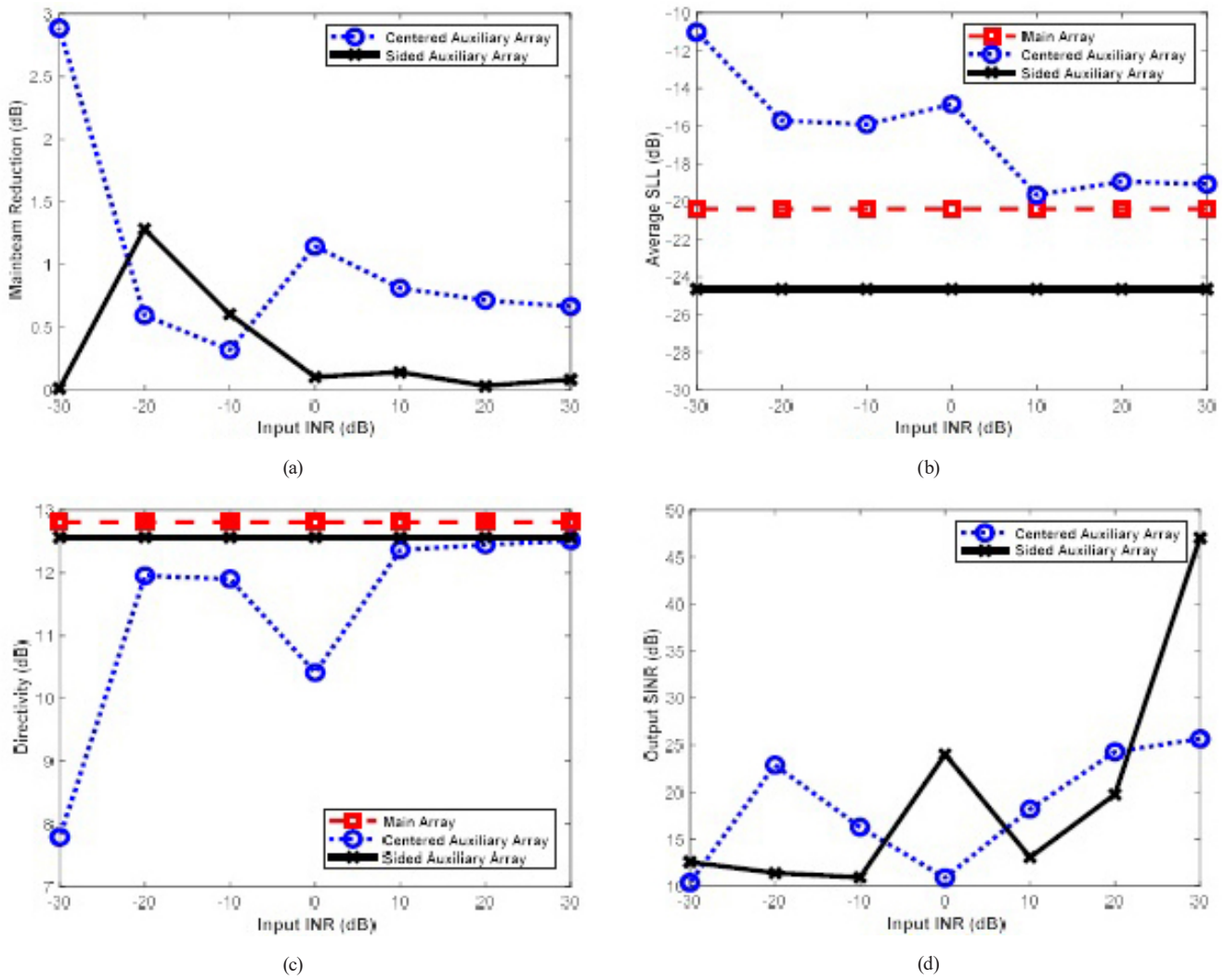


Fig. 6 Performance measures versus input interference to noise ratio, (a) main beam reduction, (b) average sidelobe level, (c) directivity, (d) output SINR

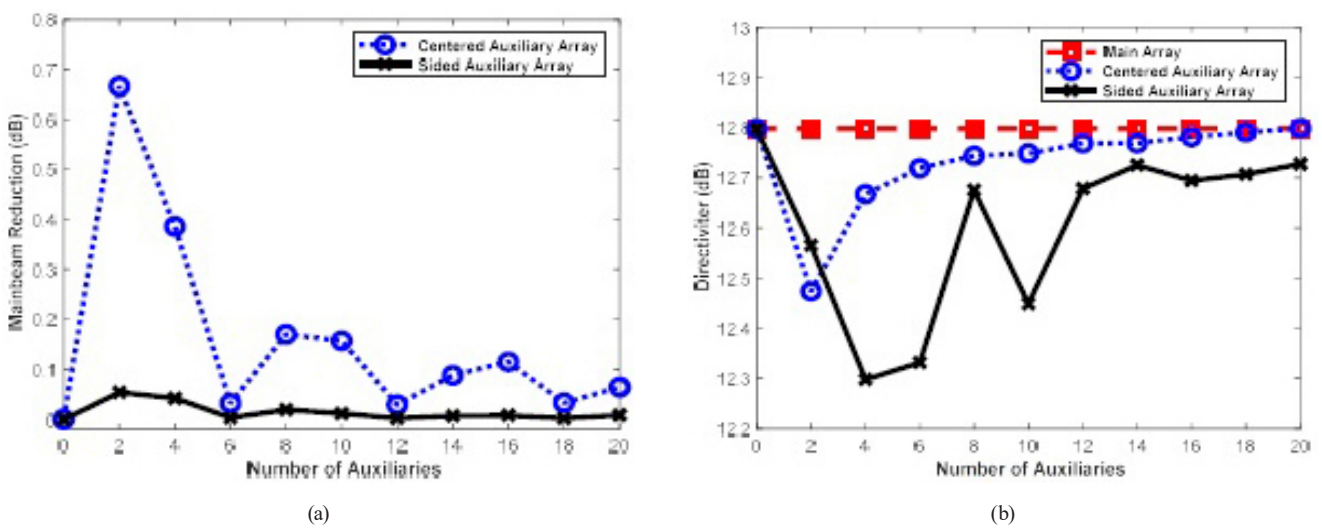
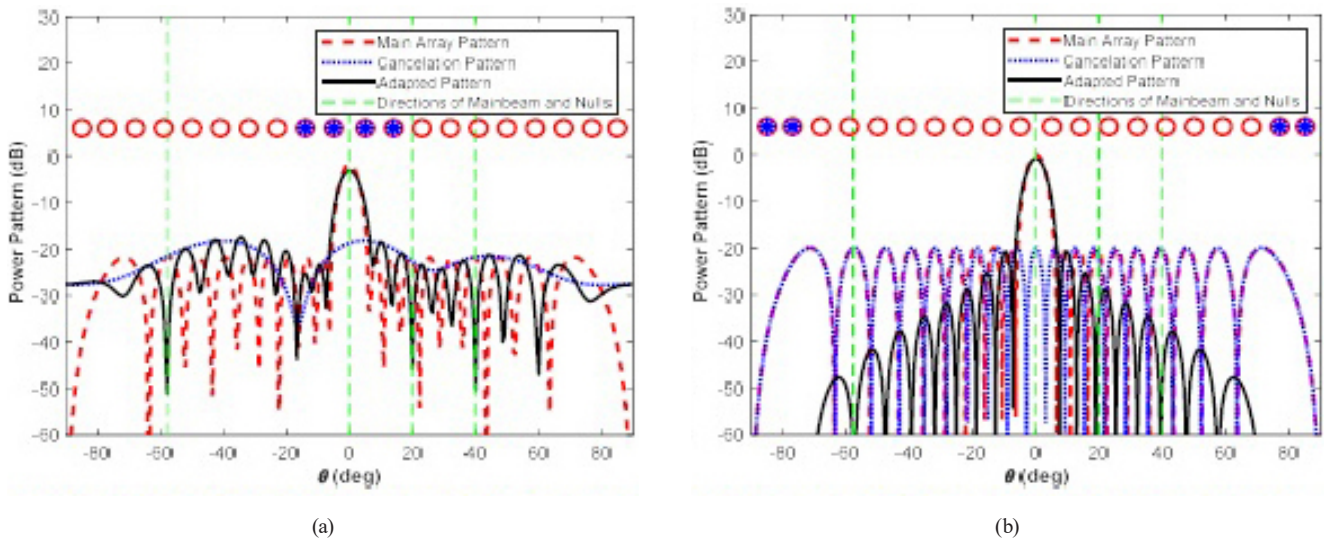


Fig. 7 Performance measures versus number of auxiliaries, (a) main beam reduction, (b) directivity

In the last example, the performances of the two modified SLC configurations under multiple interfering signals are studied.

In this example, it is assumed that the interferences are impinging on the main array from the directions  $\theta_i = [-58^\circ, 20^\circ, \text{ and } 40^\circ]$ . In this case, four auxiliary



**Fig. 8** Power patterns of the main, auxiliary and adapted arrays, for Dolph taper,  $N = 20$ ,  $M = 4$ , and multiple nulls, (a) centered-elements configuration, and (b) sided-elements configuration

elements either at the center of the main array or at the sides are reused with the adaptive control to produce the required cancellation patterns. The results are plotted in Fig. 8. It can be seen that the proposed SLC with sided-elements configuration demonstrates an appropriate operation to allocate nulls towards all the interfering directions and maintain extremely low sidelobes.

## 5 Conclusion

This study seeks to determine how the auxiliaries of the sidelobe canceller system should be selected and adaptively adjusted to attain best performance in terms of null control, low sidelobes, directivity, and lowest main beam distortion. The centered and sided elements selection have been demonstrated and it is generally found that the sided-elements configuration provides more desirable

features such as better diversity and sidelobe pattern than that of the centered-elements configuration. Further, the modified SLC could be considered as a type of partially adaptive arrays that are less complex to implement. From the simulation results, it is found that the average sidelobe level, main beam distortion, directivity, and the output SINR of the sided-elements configuration were better than those of the centered-elements configuration. Moreover, the taper efficiency of the proposed sided-elements configuration was found to be only slightly changed with compared to that of the main array. This is mainly because of the advantage of reuse only small fraction of the array elements as auxiliaries that their taper values have lowest weights at the array ends. In the future works, the proposed method may extend and applied to other array configurations such as circular or rectangular planar arrays.

## References

- [1] Weiner, M. M. (ed.) "Adaptive Antennas and Receivers", CRC Press, 2006. ISBN 9781315221151  
<https://doi.org/10.1201/9781420026498>
- [2] Compton, R. T. "Adaptive Antennas: Concepts and Performance", Prentice Hall, 1988. ISBN 978-0130041517
- [3] Frost, O. L. "An Algorithm for Linearly Constrained Adaptive Array Processing", Proceedings of the IEEE, 60(8), pp. 926–935, 1972.  
<https://doi.org/10.1109/PROC.1972.8817>
- [4] Van Trees, H. L. "Optimum Array Processing: Part IV of Detection, Estimation and Modulation Theory", John Wiley & Sons, Inc., 2002. ISBN 9780471093909  
<https://doi.org/10.1002/0471221104>
- [5] Li, J., Stoica, P. "Robust Adaptive Beamforming", John Wiley & Sons, Inc., 2005. ISBN 9780471678502  
<https://doi.org/10.1002/0471733482>
- [6] Wax, M., Anu, Y. "Performance Analysis of the Minimum Variance Beamformer", IEEE Transactions on Signal Processing, 44(4), pp. 928–937, 1996.  
<https://doi.org/10.1109/78.492545>
- [7] Cheng, X., Aubry, A., Ciuonzo, D., De Maio, A., Wang, X. "Robust Waveform and Filter Bank Design of Polarimetric Radar", IEEE Transactions on Aerospace and Electronic Systems, 53(1), pp. 370–384, 2017.  
<https://doi.org/10.1109/TAES.2017.2650619>
- [8] Ciuonzo, D., De Maio, A., Foglia, G., Piezzo, M. "Intrapulse radar-embedded communications via multiobjective optimization", IEEE Transactions on Aerospace and Electronic Systems, 51(4), pp. 2960–2974, 2015.  
<https://doi.org/10.1109/TAES.2015.140821>



- [9] Mohammed, J. R. "Design of Printed Yagi Antenna with Additional Driven Element for WLAN Applications", *Progress In Electromagnetics Research C*, 37, pp. 67–81, 2013.  
<https://doi.org/10.2528/PIERC12121201>
- [10] Mohammed, J. R. "Synthesizing Sum and Difference Patterns with Low Complexity Feeding Network by Sharing Element Excitations", *International Journal of Antennas and Propagation*, 2017, 2563901, 2017.  
<https://doi.org/10.1155/2017/2563901>
- [11] Mohammed, J. R., Sayidmarie, K. H. "Synthesizing Asymmetric Side Lobe Pattern with Steered Nulling in Nonuniformly Excited Linear Arrays by Controlling Edge Elements", *International Journal of Antennas and Propagation*, 2017, 9293031, 2017.  
<https://doi.org/10.1155/2017/9293031>
- [12] Mohammed, J. R., Sayidmarie, K. H. "Sidelobe Cancellation for Uniformly Excited Planar Array Antennas by Controlling the Side Elements", *IEEE Antennas and Wireless Propagation Letters*, 13, pp. 987–990, 2014.  
<https://doi.org/10.1109/LAWP.2014.2325025>
- [13] Mohammed, J. R. "Obtaining Wide Steered Nulls in Linear Array Patterns by Optimizing the Locations of Two Edge Elements", *AEU - International Journal of Electronics and Communications*, 101, pp. 145–151, 2019.  
<https://doi.org/10.1016/j.aeue.2019.02.004>
- [14] Sayidmarie, K. H., Mohammed, J. R. "Performance of a Wide Angle and Wide Band Nulling Method for Phased Arrays", *Progress In Electromagnetics Research M*, 33, pp. 239–249, 2013.  
<https://doi.org/10.2528/PIERM13100603>
- [15] Mohammed, J. R. "A New Simple Adaptive Noise Cancellation Scheme Based On ALE and NLMS Filter", In: *Fifth Annual Conference on Communication Networks and Services Research (CNSR '07)*, Fredericton, NB, Canada, 2007, pp. 245–254. ISBN 0-7695-2835-X  
<https://doi.org/10.1109/CNSR.2007.4>
- [16] Mohammed, J. R. "Low Complexity Adaptive Noise Canceller for Mobile Phones Based Remote Health Monitoring", *International Journal of Electrical and Computer Engineering (IJECE)*, 4(3), pp. 422–432, 2014.  
<https://doi.org/10.11591/ijece.v4i3.5534>
- [17] Mohammed, J. R., Sayidmarie, K. H. "Performance evaluation of the adaptive sidelobe canceller system with various auxiliary configurations", *AEU - International Journal of Electronics and Communications*, 80, pp. 179–185, 2017.  
<https://doi.org/10.1016/j.aeue.2017.06.039>
- [18] Balanis, C. A. "Antenna Theory: Analysis and Design", 4th ed., John Wiley & Sons, Inc., 2016. ISBN 978-1-118-64206-1